Results in Physics 15 (2019) 102617

Contents lists available at ScienceDirect

Results in Physics

journal homepage: www.elsevier.com/locate/rinp

Microarticle

Do lunar rover wheels sink equally on Earth and Moon?

A.J.R. Lopez-Arreguin[a,*], B. Gundlach[b], E. Stoll[a]

[a] Institute of Space Systems, TU Braunschweig, Hermann-Blenk-Strasse 23, Braunschweig 38108, Germany
[b] Institut für Geophysik und extraterrestrische Phyisk, Technische Universität Braunschweig, Mendelssohn Str. 3, 38106 Braunschweig, Germany

ARTICLE INFO

Keywords:
Sinkage
Wheel
Rover
Gravity
terramechanics

ABSTRACT

There has been a long discussion on how the low-gravity effects that LRUs (Lightweight Rover Units) on the Moon will experience, can affect mission planning and surface operations. In particular, the sinkage observed when regolith soil layers collapse under a normal wheel load has been an important source of contradiction in the field of Terramechanics in the last years. In this short report we review the different authors opinions on this topic, examining in detail their definition, methods, and results.

The sinkage of static wheels under lunar gravity could be less than on Earth (fixing body dimensions and soil), given the decreased normal load experienced by loose regolith. This is known as static sinkage. On the other hand, if the wheels are in permanent rotation, the effect of poor soil's bearing capacity in lower gravities can lead to a deeper intrusion of the wheels as compared to the case on Earth (dynamic sinkage). The dynamic and static sinkage are low in lunar gravity and have more or less similar values in case the wheel surface is plane (smooth). However, if the wheel under test incorporates grousers, the lugs motion and soil's bearing capacity would make the separate effect of dynamic sinkage to be much larger than in plane wheels. Finally, we evaluated a method that (at difference from previous models), can express more accurately the effect of static and dynamic sinkage in different gravity environments. The novel semi-empirical approach to estimate wheel penetration into soils assumes a dependency from wheel parameters, slip and terrain mechanical properties, demonstrating an improved goodness-of-fit (R^2) from 91 to 99%, distinctly in a gravity interval of $\frac{1}{6}$ up to 2 times the gravity on Earth.

Introduction

One of the most important tasks for the exploration of other planetary surfaces is to guarantee the survival of the deployed technology. In particular, in order to accomplish in situ tasks on other celestial bodies than Earth, we must deploy autonomous surface robots capable to achieve demanding tasks while traveling on unknown terrain. To improve the robustness of any planetary mission, we must therefore understand the mobility of such machinery typically embodied in wheeled rovers. The Terramechanics field of engineering is a key element to reveal how granular soils and wheel configurations interplay allowing rovers to travel without any conflict caused by the natural restrictions of the terrain. Using the approach of such field study, rover wheels are tested individually to reveal their forces, stresses, sinkage and torques based on onboard sensors embedded in the wheel unit [1]. That way those physical parameters can be assessed in real time and compared with analytical models previously formulated, providing important insights how the rover will behave as a complete system. It is very important to highlight, that among all physical variables determinable through experiments, the wheel penetration distance into the soil is the most visible element and defines whether a rover can continue moving functionally. Previous research has shown that the Mars exploration rover (MER) Spirit was stuck while transversing highly deformable sulfate-rich soils, for which the compaction resistance is very low allowing soil failure with a minimum exerted load and making wheels to penetrate very easily [2,3]. The Opportunity rover on the other hand also experienced high wheel sinkage levels while crossing wind-blown ripples [4]. Thus, predictions of wheel sinkage is a subject of ongoing research. Given the sum between the initial and final sinkage is known as total sinkage z_T, at the present state of the art some teams [5] claim that the observable z_T rover wheels could experience on Earth (z_E), is the same as the one we could measure on another planetary bodies, z_{ex} (i.e. $z_{ex} = z_E$), eventually even in presence of a different gravity field than present on Earth (keeping actual wheel dimensions, wheel mass and terrain invariant). In particular, Kobayashi and his team tested their claims during different parabolic flight campaigns, with the final conclusion that the field level has no effect on the wheel's sinkage [5]. In contrast, different field

* Corresponding author.
E-mail address: amenosis.lopez@tu-braunschweig.de (A.J.R. Lopez-Arreguin).

https://doi.org/10.1016/j.rinp.2019.102617
Received 25 March 2019; Received in revised form 2 August 2019; Accepted 26 August 2019
Available online 29 August 2019

studies differ in their results (e.g. [6,7]), suggesting rover wheels could display worst sinkage performance in lower gravity fields than Earth, due to the soil strength reduction. Therefore with this study we intend to shine a light into this topic. For this purpose, we re-examine the previous data of Kobayashi's parabolic flights [5], scrutinizing the different author's views and definitions in subsequent studies with the use of (newer) high accuracy terramechanics models able to predict wheel sinkage in granular soils within 10^{-6} m [8]. As previously mentioned no variations in the z_T were discerned as function of gravity only, thus no terramechanics models have been validated to date to assess sinkage in complex environments different than Earth. Thus, we review the range of applicability of typical sinkage estimation methods considered in the literature over different gravity domains, proposing a parallel semi-empirical description that incorporates the basic physics of the interaction. Modeling of the wheel's sinkage in soils and experiments on Earth will be addressed in Section "Vehicle terrain interaction". Section "Measurements and discussion" extends the theoretical models to different gravity regimes.

Vehicle terrain interaction

Modeling sinkage

In static conditions, the pressure P exerted by the loose soil over a sinking flat plate surface can be approximated as power law of its depth of penetration z [9,10]:

$$P(z) = k\, z^n \tag{1}$$

where k is known as the sinkage modulus and has units in [Pa/m^n], while the sinkage exponent n is dimensionless. Both are terrain-related parameters which are characterized with a minimum of two penetrometer tests with different plate widths or radii [10]. In the case of wheels lying in loose soils, the ground is compressed by the circumference of a wheel of radius r. It was Bekker [11] who noticed that for typical rigid wheels ($r > 0.25$ m), the contact with the soil can be assumed to be a flat area. For smaller wheels Eq. (1) still valid modulating the values for n [12] (this will be amply discussed in next section). Fig. 1 shows a wheel sinking into the soil with a load W. Notice the sinkage at the front and the rear are approximately equal only if the wheel is static. If the wheel is driving, the contact angle in the rear part will be lower, similarly as depicted by the figure. The differentials dN represent the elementary reactions perpendicular to the circumference of the wheel that act against rolling (any reactions tangent to the wheel surface can be ignored because are very small [11]). The vertical forces in the wheel's center of mass can be derived by bare integration of the differentials acting on the plane described by Fig. 1 [13,14]:

$$W = \int_{\theta_2}^{\theta_1} dN \cos\theta + \int_{\theta_2}^{\theta_1} dF_\phi \sin\theta \tag{2}$$

As assumed before, for a static wheel the elemental shear reactions are very low ($dF_\phi \approx 0$), whereas for a dynamic wheel, the second right-hand term of Eq. (2) cannot be neglected [8]. Given the distances from the origin to the point of action of the elementary reactions dN are $x = r\sin\theta$ and $z(\theta) = r(\cos\theta - \cos\theta_1)$ [11], θ is the contact angle and θ_1 is the entrance angle, and the instantaneous differentials can be given by $dx = r\cos\theta\, d\theta$, $dz = -r\sin\theta\, d\theta$. Thus we can relate the normal force components which are simply $dN\sin\theta = P(z)\, b\, dz$ and $dN\cos\theta = -P(z)\, b\, dx$, where b is the wheel width. This way the following expression is obtained from integration of Eq. (2) [14]:

$$W \approx N_z|_{-\theta_1}^{\theta_1} = \frac{2bk_s z_o^{n+1}}{\theta_1} \approx \sqrt{D}\, bk_s z_o^{n+\frac{1}{2}} \tag{3}$$

That can be arranged to solve for the sinkage:

$$z_0 = \left(\frac{W}{\sqrt{2r}\, b\, k}\right)^{1/(n+1/2)} \tag{4}$$

On the other hand, the traditional Bekker analytical model for estimating the wheel sinkage can be derived in similar form [11]:

$$z_0 = \left(\frac{3W}{\sqrt{2r}\, b\, k\,(3-n)}\right)^{1/(n+\frac{1}{2})} \tag{5}$$

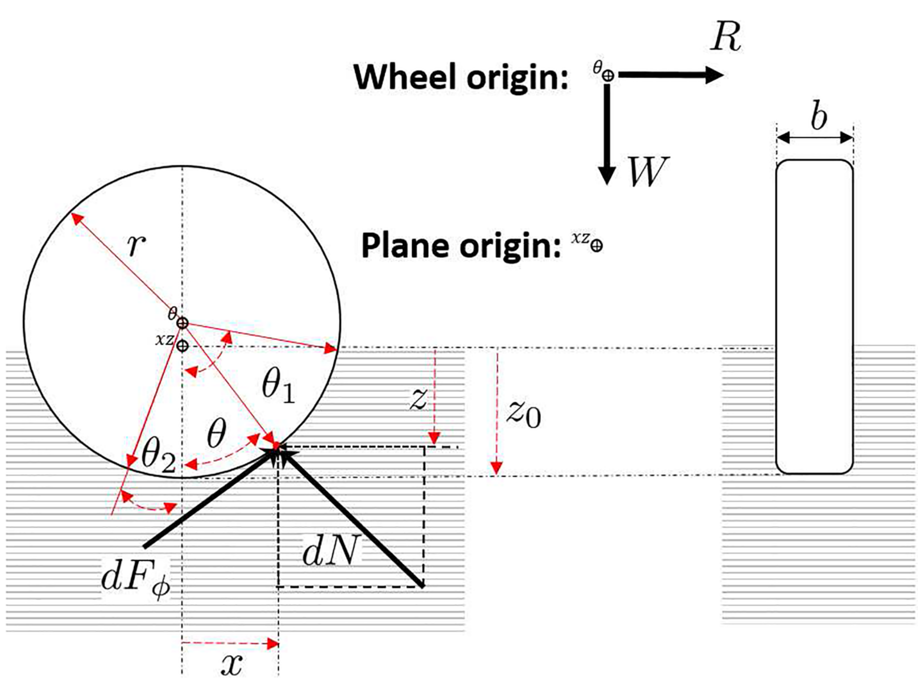

Fig. 1. Sinkage of a wheel of radius r. Notice the entrance angle θ_1 and the exit angle θ_2, whom are incorporated from the Wong-Reece model of terramechanics [14]. Notice also the pulling force in the horizontal direction equals the movement resistance R. A better understanding of the model here presented can be addressed in [14].

Notice in both expressions for static sinkage, the magnitude depends explicitly on the wheel load, radius, width and terrain-related mechanical properties (k, n). To improve the accuracy of previous formulas for z_0 the following section discusses most of the semi-empirical approaches adopted in distinct terramechanics studies on Earth. Although terrain parameters in lunar environment can be estimated via in situ penetrometer tests (e.g. as those of Lunokhod [15]).

Semiempirical approach

In order to comprehensively understand the process of wheel penetration, we need to differentiate among static and dynamic sinkage. Even both situations are the result of the soil collapse under a normal load, the first is measured at the inital time of contact and the second is only measured while the wheel rotates. Thus, we can establish that:

$$z_T = z_0 + z_d \tag{6}$$

with z_0 the static sinkage and z_d the dynamic sinkage. The k and n parameters implicit in sinkage formulae (and derived from Eq. (1)), are semi-empirically obtained by fitting data of soil's experiments, thus they are not intrinsic terrain parameters. Generally Eq. (1) may be improved upon modulating the sinkage exponent and modulus accordingly, to charactacterize the pressure-sinkage curve more precisely. The typical approach is to fix a constant k for every type of soil, and modifying the sinkage exponent n according the nature of experiment [12]. In particular, to predict the static sinkage with variation of the normal load, the sinkage exponent n reads [8]:

$$n = n_0 + n_1 W \tag{7}$$

where n_0 is the constant value derived by direct soil testing, and n_1 a fitting constant. On the other hand, notice in loose soils a driving wheel will slip generally. Thus in dynamic conditions z_d can be approximated as function of the slip ratio s according to [14]:

$$n = n_0 + n_2 s \tag{8}$$

In Eq. (8), n_2 is a fitting parameter and s is function of the wheel longitudinal velocity v and their angular speed ω:

$$s = 1 - \frac{v}{r\omega},\ (|r\omega| \geqslant |v|)\text{: driving} \tag{9}$$

The dependence of the sinkage on the slip ratio is well know in the field. In summary, formulas like Eqs. (5) or (4) are the typical estimators of sinkage in Terramechanics, and can be used for z_0 or z_d varying the sinkage exponent among: (i) a constant value $n = n_0$; (ii) a variable value including the influence of the load as expressed by Eq. (7); (iii) as function of the slip only in cases wheels are driving. This is presented in Table 1, where we arranged M1 to M4-labeled models for static sinkage, while M5 and M6 models for dynamic sinkage. The remaining models M7-M8 in the table will be introduced later.

Measurements and discussion

Static sinkage in partial gravities

In order to relate the sinkage with the gravity we use the formulation of k given by the Reece formulation[16]:

$$k = K_c + K_\phi G \tag{10}$$

where the constants are taken from soil penetration tests in Earth are [17]: $K_c = \frac{1370}{b}$ Pa/m^n and $K_\phi = \frac{814 \cdot 10^3}{G}$ Pa/m^{n-1}s^{-2} (set for FJS-1 lunar simulant soil). Using Eq. (5) and (10), we can relate the ratio of the static sinkage measured on Earth z_{Eo} to the static sinkage in a distinct gravity environment z_{exo}, by:

$$z_{exo}/z_{Eo} = \frac{\left(\frac{3W_{ex}}{b(3-n)(K_c + K_\phi g_{ex})\sqrt{D}}\right)^{2/(2n+1)}}{\left(\frac{3W_E}{b(3-n)(K_c + K_\phi G)\sqrt{D}}\right)^{2/(2n+1)}} \tag{11}$$

where $W_{ex} = m_{ex} g_{ex}$ and $W_E = m_E G$ (m_{ex} and m_E are the wheel body mass in a partial gravity environment and on Earth, respectively). Notice we have that K_ϕ and n are independent of G [18]. K_c usually attain very low values when regolith is very dry and low in cohesion (such as Moon or Mars regolith). Simplifying Eq. (11), Wong [18] proposed that wheels with identical mass, obey the following rule:

$$z_{exo}/z_{Eo} = \left[\frac{m_{ex}}{m_E}\right]^{2/(2n+1)} = 1 \tag{12}$$

Now let's look at the experimental results. The recorded values of static

Table 1
Terramechanics semi-empirical models to estimate the sinkage.

Represented Sinkage z	Model	Baseline Equation	Model source author
Static (z_0)	M1	$z = \left[\frac{3W}{\sqrt{2r}\,b\,k\,(3-n_0)}\right]^{1/(n_0+\frac{1}{2})}$	[11]
Static (z_0)	M2	$z = \left[\frac{W}{\sqrt{2r}\,b\,k}\right]^{1/(n_0+\frac{1}{2})}$	[8]
Static (z_0)	M3	$z = \left[\frac{3W}{\sqrt{2r}\,b\,k\,(3-n_0-n_1 W)}\right]^{1/(n_0+n_1 W+\frac{1}{2})}$	[8]
Static (z_0)	M4	$z = \left[\frac{W}{\sqrt{2r}\,b\,k}\right]^{1/(n_0+n_1 W+\frac{1}{2})}$	[8]
Dynamic (z_d)	M5	$z = \left[\frac{3W}{\sqrt{2r}\,b\,k\,(3-n_0-n_2 s)}\right]^{1/(n_0+n_2 s+\frac{1}{2})}$	[14]
Dynamic (z_d)	M6	$z = \left[\frac{W}{\sqrt{2r}\,b\,k}\right]^{1/(n_0+n_2 s+\frac{1}{2})}$	[14]
Dynamic (z_d)	M7	$z = \left[\frac{3W}{\sqrt{2r}bk(3-n_0-n_2 s-n_3 W)}\right]^{1/(n_0+n_2 s+n_3 W+\frac{1}{2})}$	Proposed
Dynamic (z_d)	M8	$z = \left[\frac{W}{\sqrt{2r}bk}\right]^{1/(n_0+n_2 s+n_3 W+\frac{1}{2})}$	Proposed

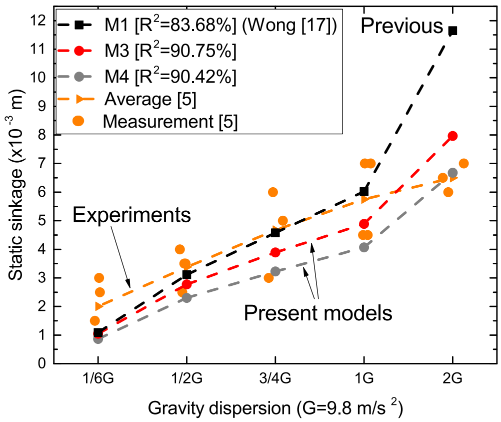

(a) Static sinkage for FJS (D_r = 50%)

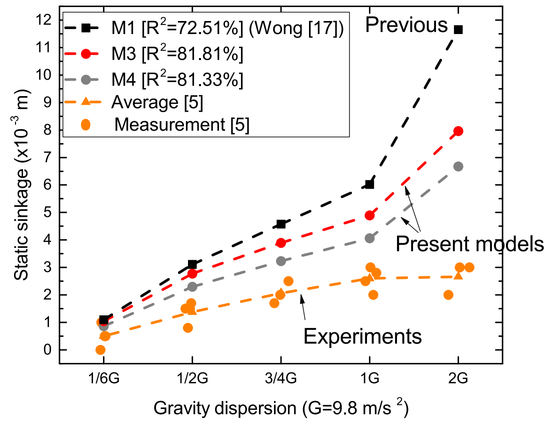

(b) Static sinkage for FJS (D_r = 75%)

Fig. 2. Static sinkage behavior over different gravities for FJS with density 50%, recorded during parabolic flights for a wheel with r = 75 mm and b = 80 mm, subjected to a normal mass of m = 10 kg [5]. For the analytical models, n_0 = 0.55 and n_1 = −3.89 * 10^{-4} were used.

sinkage versus partial gravities from Kobayashi [5] (in FJS simulant soil of two relative densities D_r), are presented in Fig. 2, along with previous modeling of Wong, named as M1 [18]. It can be seen that the static sinkage shows fluctuations (in the order of 10^{-3} m), that are very small and difficult to monitor on an actual rover commission. Thus previous authors omitted their interpretation (e.g. [18–20]), somehow considering Eq. (12) is always fulfilled (if $z_{exo} = z_{Eo}$, curves in Fig. 2 are such small are essentially constant). Given measurement errors are very low compared to the overall wheel displaced measurements (measurement is $\approx 2{\cdot}10^{-4}$ m [5]), our interpretation of the data in Fig. 2 is different. Namely, the lower z_0 values are linked to smaller gravity regimes. This can be understood by the following thought experiment. There are two competing effects that are essentially different with varying gravity and that balance the static sinkage. Assume that we have an object of any shape resting on loose soil, and we reduce the gravity while keeping the object mass constant.

We can perhaps conclude in this conditions the sinkage could decrement, due to a lower normal load experienced by the soil. However, a competing role is played by the terrain at the same time, as the confinement stress of the soil is reduced due to gravity, diminishing the bearing capacity the granular material can endure [6] (this event alone is the consequence of a reduction of soil's strength with lower gravities). Later, the quoted effects determine z_{exo} in partial gravities: the Reduced Normal Load (RNL) and the Reduced Bearing Capacity (RBC). They can be correlated and compared to Earth's measurements. If $z_{exo} = z_{Eo}$, none of the effects is predominant, and they cancel out maintaining the same sinkage than the observed on Earth (sinkage will not be affected by gravity change, just as Eq. (12) suggests). If $z_{exo} > z_{Eo}$, the RBC role of the soil is predominant, producing soil failure with a minimum exerted load such that the object go deeper into the soil. If $z_{exo} < z_{Eo}$, the RNL event will be dominating most of the sinkage displacement, as the load is decreased such amount the soil can resist the insertion. Therefore, from the behavior of static sinkage presented in Figs. 2 (a) and (b), can be concluded that the RNL effect is the main cause for the effect that static wheels are vertically displaced less in low gravities than at higher G's. Please mind that the dynamic sinkage does not need to follow the same rule. In fact, Jiang et al. [6] and Li et al. [7], observed a leading role of RBC effect in the Moon surface, in case of rotating wheels (this will be addressed in following Sections "Dynamic sinkage in partial gravities" and "A different approach: computational results for sinkage in space gravity environments"). Thus, we highlight the different processes that determine the total sinkage z_T as function of z_0 and z_d are not trivial. Even when those effects were not discussed in detail by the previous authors, here we can confirm that using more accurate modeling to deal with the problem. Expressing the sinkage exponent as function of the normal load (Eq. (7)), models M3 and M4 previously used for static wheels under Earth gravity [8], improve the goodness-of-fit R^2 from Wong's for both soils used (from 83 % up to 90.75 % with D_r = 50%).

Dynamic sinkage in partial gravities

In the original proposition of Wong [18], in Eqs. (11) and (12) the values z_{exo} and z_{Eo} were used as measures of the total sinkage. However, the sinkage exponent n in such formulas do not reflect any slipping of the wheels, as n is set by a constant value n_0 only (shown in M1 of Table 1). Thus, this model will not be able to predict dynamic conditions. Consequently, this section aims at emend this modeling error by proposing a more sophisticated formulation for dynamic sinkage, and re-examining the total sinkage z_T with separate analysis for z_d. In addition to the slip, modeling dynamic sinkage with varying gravity requires to involve the normal load W within the sinkage exponent n, such higher modeling fidelity can be guaranteed (as achieved before for static sinkage, with models M3 and M4 in Fig. 2). Thus we propose:

$$n = n_0 + n_2 s + n_3 W \tag{13}$$

with n_0 and n_2 as defined in Section "Vehicle terrain interaction", and n_3 a new fitting constant. The models derived from Eq. (13) have been arranged into Table 1 as M7 and M8. They are compared to z_T results coming from Kobayashi's parabolic flights [5], in Figs. 3 (a)-(e), as function of the slip ratio s_{ex} and gravity for soil density D_r = 50%. Models M7 and M8 can reproduce experimental results with an accuracy varying from 91.5 to 99.7% (M7), and from 91.01–99.8% (M8) in the interval $G \in (\frac{1}{6}, 2)$.

In a further study [19], Wong and Kobayashi came up with a simple relation for slip-sinkage data, standing on a fitting by least squares for each g_{ex}:

$$z_{ex} = a\, s_{ex} + y \tag{14}$$

where a and y are fitting parameters. In all cases the previous Eq. (14)

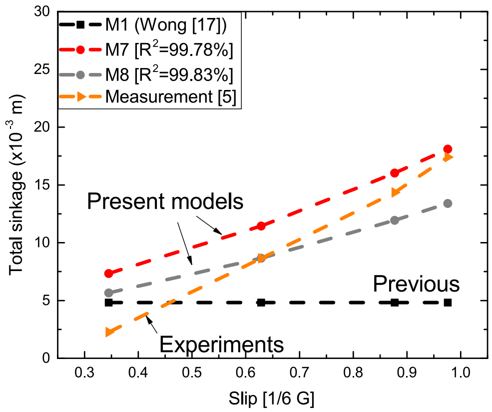

(a) Total sinkage at 1/6G

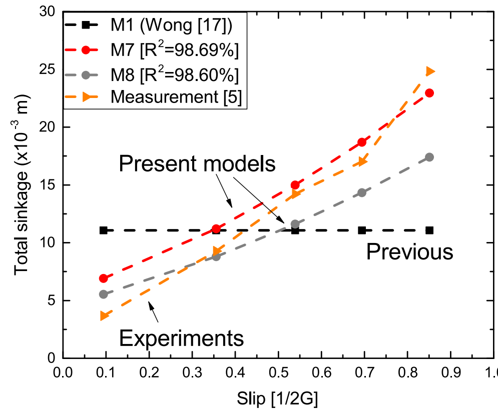

(b) Total sinkage at 1/2G

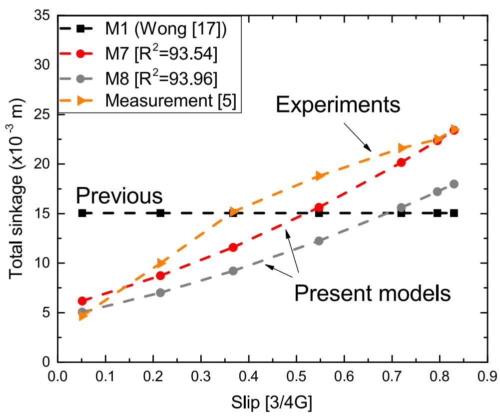

(c) Total sinkage at 3/4G

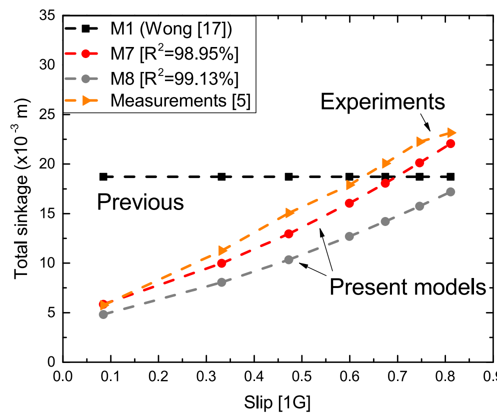

(d) Total sinkage at 1G

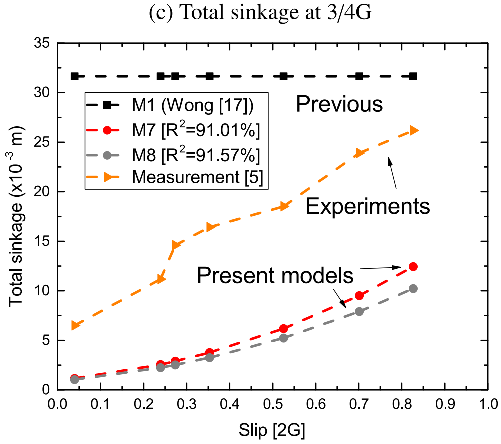

(e) Total sinkage at 2G

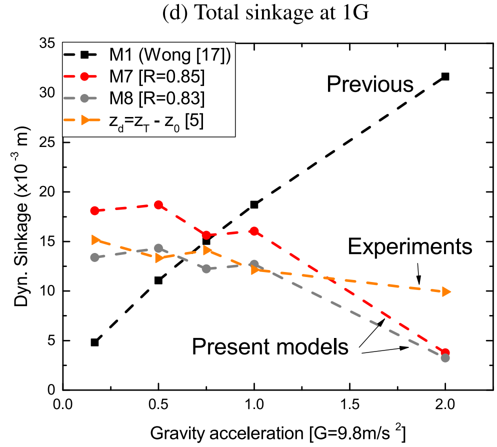

(f) Dynamic sinkage at 1/6G-2G

Fig. 3. Measured and modeled dynamic sinkage z_d in partial gravity environments for FJS at 50% of relative density. In all cases the slip ratio and the time can be related as similar metrics (the slip increase according time). For the analytical models, the constant values of $n_0 = 0.82$, $n_2 = 0.45$ and $n_3 = -3.2 \cdot 10^{-3}$ were used. The rotation itself makes wheels to penetrate more into the soil, where the soil failure expands everytime additional torque is provided to maintain a constant wheel angular speed. Thus the experimental z_T (and consequently, the dynamic sinkage $z_d = z_T - z_0$) always increase with time regardless the gravity level.

shown an excellent goodness-of-fit (R^2 up to 98%). However, the main drawbacks of sinkage prediction with Eq. (14) are: (a) there is a unique set of parameters a and y that need to be derived by a series of tests over each partial gravity, thus formulation cannot be adapted to any gravity higher or lower than g_{ex}. In contrast, Eq. (13) is applicable to varying gravity with the same set of constants (n_0, n_2 and n_3). (b) It is a sole equation that does not depend on any physical parameter like the wheel geometry or the soil properties, making difficult to be used for different wheel configurations or extrapolated to another soils. Our proposed methods M7 and M8 based in Eq. (13), depend explicitly on the slip ratio, wheel mass and width, gravity and other terrain-related parameters defined in the k modulus.

Finally, Fig. 3 (f) display the dynamic sinkage versus gravity acceleration. The values (calculated from Eq. (6)) shown z_d is always greater in lower gravity levels, in opposite form as for the static sinkage. That means, that compared to Earth the wheel performance would be significantly degraded in lunar conditions due to higher sinkage. This fulfills the observations from [6], in a way that when rotated, wheels could slip more in low G's due to the poor soil strength with decreased gravity (in case the same soil is used and other conditions as previously assumed). The analysis is further extended changing the relative density of the soil to $D_r = 70\%$, and measuring the outcomes of the sinkage. The plots are presented in the Annex. The accuracy of the present models M7-M8 is proved to be high under change in terrain density, eventually without varying the set of constants n_0, n_2, and n_3 previously calibrated. The R^2 term for model M7 varies within 80.09 to 97.59% for FJS ($D_r = 70\%$), and for M8 within 81.14 to 97.86%. The experimental z_d could be verified by modeling with a precision better than 91% with $D_r = 70\%$. Thus models M7-M8 were validated.

A different approach: computational results for sinkage in space gravity environments

The wheel behavior in low gravity environments have been the subject of extensive studies using computational tools based in the discrete element method (DEM), a modern approach to address many-body physical systems whom equations are difficult to compute analytically. Providing a broad overview on the subject of numerical modeling of wheels in loose soils is out of the scope of this brief research. However, given the importance of studies to date on the field, here we mention the few ones dealing with investigation of mobility over diferent gravities. Nakashima et al. [20], employing a DEM code able to simulate flow of particles in two dimensions (2D-DEM code), complemented the results of Kobayashi's parabolic flights (presented in Sections "Static sinkage in partial gravities" and "Dynamic sinkage in partial gravities"). They used a single plane wheel and two distinct virtual soils calibrated with similar properties of FJS and Toyura [21,20], subjected distinct gravity accelerations. Their concluding remark is that the amount of wheel penetration in the soil (keeping terrain and wheel fixed) does not vary with gravity. However, in the reported sinkage values and analysis presented by the group of Nakashima, it is not addressed the distinction among static or dynamic sinkage phenomenon. Further, results are not conclusive regarding different wheel design other than plane wheels (e.g. wheels with grousers) could be employed [20]. Lugged wheels were numerically tested over distinct gravity regimes by Knuth et al. [22], Jiang et al. [6] and Li et al. [7], in particular to a lunar gravity level. Only the later two authors reported their sinkage performance. Such observations manifest that: (a) wheels with grousers have larger z_d variations that the one we can observe in the present analysis with plane wheels, and (b) z_d is always larger on the Moon than on Earth, due to LBC effect [6]. In that case, models M7-M8 shall be sufficiently robust to predict the dynamic sinkage according the terrain, slip and net load, only by changing the fitting constants of the model. Giving the lack of explicit z_0 and z_T results from the later reports, proving semiempirical models M7-M8 with DEM analysis can be subject of a further study.

Conclusions

One of the most remarkable examples of the success of Bekker's theory set in 1957 is that made up much of what we know about trafficability of rovers in extraterrestrial terrains. Eventually their formulas although originally applicable to Earth, have presented improvements that condensed the need to provide more accurate metrics to the physical magnitudes observed during experiments. To the current question whether the newest models to date can find applications in the work of prediction in different places than Earth, the description provided here highlights there is no present way to estimate the wheel sinkage as function of the gravity level with accuracy, based in bare terramechanics formulas. Here we begin detailing there exist two different processes associated with the wheel penetration on soils in extraterrestrial terrains, for which the static sinkage needs a closer look to define whether the bearing capacity of the soil or the normal load play a predominant role. Even the dynamic sinkage is essentially low, their variation with slip could allow us to observe the bearing capacity of the soil gets worsen the lower the gravity is. Further, previous observations on Earth have shown z_d tends to increase with addition of lugs onto the wheels, and numerical experiments at lunar gravity level have indicated that z_d is essentially larger on the Moon than on Earth. In any case, the models proposed here show an improved goodness-of-fit (R^2) regarding experimental data, and a G-dependency (while older models are not G-dependent). The goodness-of-fit are better than 91% for both models here tested ($M7$, $M8$). The physics of the wheel-soil interaction is accounted, which will provide the possibility to reproduce or extrapolate the present models to different soil properties or wheel geometries. Although typical rovers traversing in open terrains may present a time variation of the slip, detecting this parameter may not be as easy as in laboratory conditions. In particular, vision based algorithms can be used to detect the vehicle speed [23], and wheel encoder information can allow estimation of the slip. On the other hand, wheel sinkage can also be detected by processing image data [24].

Acknowledgments

We acknowledge Prof. Taizo Kobayashi for his kindness and support sharing his original data of parabolic flights and earth-based experiments. The authors also thank to Prof. Anton Kulchitsky for his valuable comments to the realization of this manuscript. This work was supported by the Project No. ZW 6-85007621, funded by Europäischer Fonds für regionale Entwicklung (EFRE). The authors thank the computational resources provided by Thubath-Kaal HPC Center.

Annex

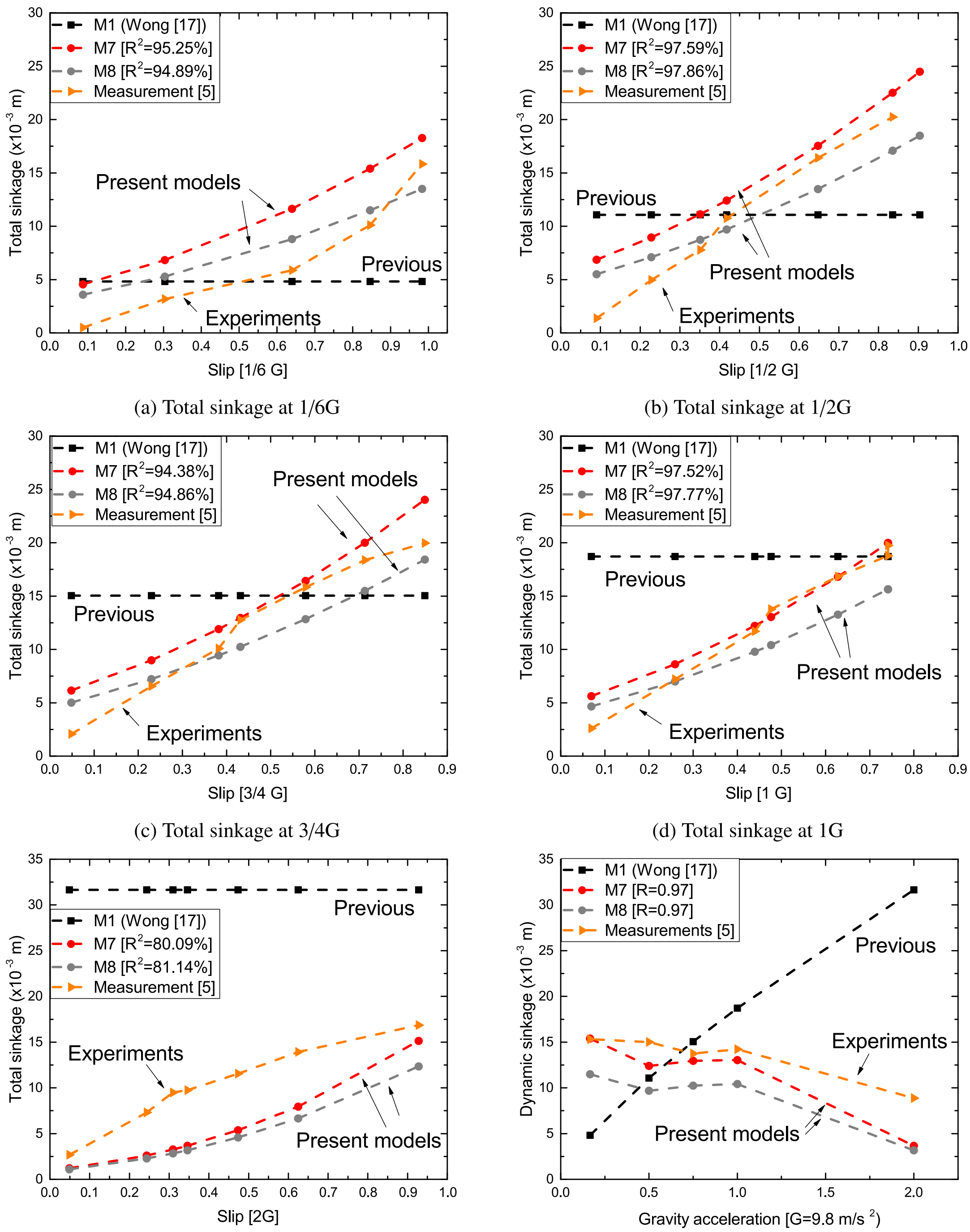

(a) Total sinkage at 1/6G

(b) Total sinkage at 1/2G

(c) Total sinkage at 3/4G

(d) Total sinkage at 1G

(e) Total sinkage at 2G

(f) Dynamic sinkage at 1/6G-2G

Fig. 4. Measured and modeled dynamic sinkage z_d in partial gravity environments for FJS at 70% of density. For the analytical models essentially the same sinkage exponent constants than for FJS at $D_r = 50\%$ were employed ($n_0 = 0.82$, $n_2 = 0.45$ and $n_3 = -3.2 * 10^{-3}$).

References

[1] Siciliano B, Khatib O. Springer handbook of robotics. Springer; 2016.

[2] Johnson JB, Kulchitsky AV, Duvoy P, Iagnemma K, Senatore C, Arvidson RE, et al. Discrete element method simulations of mars exploration rover wheel performance. J Terramech 2015;62:31–40.

[3] Arvidson RE, Bell III JF, Bellutta P, Cabrol NA, Catalano J, Cohen J, et al. Spirit mars rover mission: overview and selected results from the northern home plate winter haven to the side of scamander crater. J Geophys Res: Planets 2010;115(E7).

[4] Zhou F, Arvidson RE, Bennett K, Trease B, Lindemann R, Bellutta P, et al. Simulations of mars rover traverses. J Field Robotics 2014;31(1):141–60.

[5] Kobayashi T, Fujiwara Y, Yamakawa J, Yasufuku N, Omine K. Mobility performance of a rigid wheel in low gravity environments. J Terramech 2010;47(4):261–74.

[6] Jiang M, Liu F, Shen Z, Zheng M. Distinct element simulation of lugged wheel performance under extraterrestrial environmental effects. Acta Astronautica

2014;99:37–51.
[7] Li W, Huang Y, Cui Y, Dong S, Wang J. Trafficability analysis of lunar mare terrain by means of the discrete element method for wheeled rover locomotion. J Terramech 2010;47(3):161–72.
[8] Ding L, et al. Improved explicit-form equations for estimating dynamic wheel sinkage and compaction resistance on deformable terrain. Mech Mach Theory 2015;86:235–64.
[9] Bekker MG. Off-the-road locomotion: research and development in terramechanics. University of Michigan Press; 1960.
[10] Wong JY. Theory of ground vehicles. John Wiley & Sons; 2001.
[11] Bekker MG. Theory of land locomotion. University of Michigan Press; 1956.
[12] Ding L, Gao H, Deng Z, Li Y, Liu G. New perspective on characterizing pressure–sinkage relationship of terrains for estimating interaction mechanics. J Terramech 2014;52:57–76.
[13] Wong JY, Reece A. Prediction of rigid wheel performance based on the analysis of soil-wheel stresses part i. performance of driven rigid wheels. J Terramech 1967;4(1):81–98.
[14] Ding L, Deng Z, Gao H, Tao J, Iagnemma KD, Liu G. Interaction mechanics model for rigid driving wheels of planetary rovers moving on sandy terrain with consideration of multiple physical effects. J Field Robotics 2015;32(6):827–59.
[15] Chhaniyara S, Brunskill C, Yeomans B, Matthews M, Saaj C, Ransom S, et al. Terrain trafficability analysis and soil mechanical property identification for planetary rovers: A survey. J Terramech 2012;49(2):115–28.
[16] Reece AR. Principles of soil-vehicle mechanics. Proc Inst Mech Eng: Autom Div 1965;180(1):45–66.
[17] Jia Z, Smith W, Peng H. Terramechanics-based wheel–terrain interaction model and its applications to off-road wheeled mobile robots. Robotica 2012;30(3):491–503.
[18] Wong JY. Predicting the performances of rigid rover wheels on extraterrestrial surfaces based on test results obtained on earth. J Terramech 2012;49(1):49–61.
[19] Wong JY, Kobayashi T. Further study of the method of approach to testing the performance of extraterrestrial rovers/rover wheels on earth. J Terramech 2012.
[20] Nakashima H, Kobayashi T. Effects of gravity on rigid rover wheel sinkage and motion resistance assessed using two-dimensional discrete element method. J Terramech 2014;53:37–45.
[21] Nakashima H, Fujii H, Oida A, Momozu M, Kanamori H, Aoki S, et al. Discrete element method analysis of single wheel performance for a small lunar rover on sloped terrain. J Terramech 2010;47(5):307–21.
[22] Knuth MA, Johnson J, Hopkins M, Sullivan R, Moore J. Discrete element modeling of a mars exploration rover wheel in granular material. J Terramech 2012;49(1):27–36.
[23] Ishigami G, Nagatani K, Yoshida K. Slope traversal controls for planetary exploration rover on sandy terrain. J Field Robotics 2009;26(3):264–86.
[24] Brooks CA, Iagnemma KD, Dubowsky S. Visual wheel sinkage measurement for planetary rover mobility characterization. Autonomous Robots 2006;21(1):55–64.